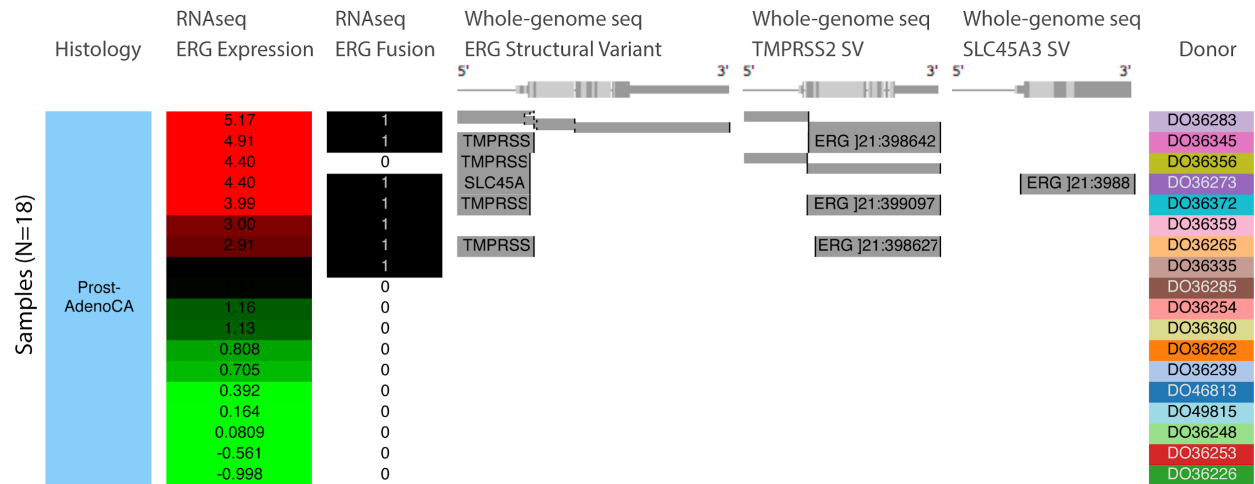


Supplemental Figures

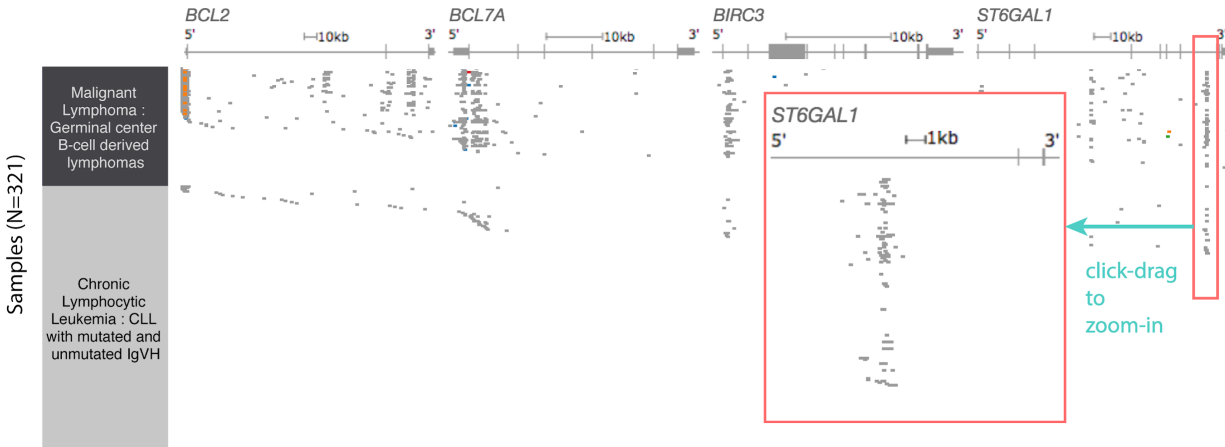
Supplemental Figure 1



Supplemental Figure 1. Visualization of large structural variants. This figure shows the frequent ERG fusion in PCAWG prostate cancer detected by both RNA-seq and DNA-seq analysis. Columns, starting at the left, correspond to histology, ERG gene expression, and ERG fusion based on RNA-seq data. Gene expression is colored red to green for high to low expression. In the ERG fusion column samples that have a fusion are marked with 1 and those that do not are marked with 0. The next three columns show structural variant calls made using whole-genome DNA-seq data for ERG, TMPRSS2, and SLC45A3. Precise breakpoints are mapped to gene annotations. A grey bar indicates an external piece of DNA that is fused at the breakpoint. Gene names on the grey bars show the origin of the external DNA that is joined. This figure shows that TMPRSS2 and SLC45A3 are fusion partners for ERG, and that these fusions correlate with over-expression of ERG. Fusions detected by RNA-seq and whole-genome sequencing are not always consistent. Here, even using a consensus of DNA-based detection methods, one fusion detected by a consensus of RNA-based detectors is missed, and the converse is also seen. This example shows that an integrated visualization across multiple data types and algorithms provides a more accurate model of a genomic event.

<https://xenabrowser.net/heatmap/?bookmark=24ad428d0f3bf3bf3205bcffab64d276>

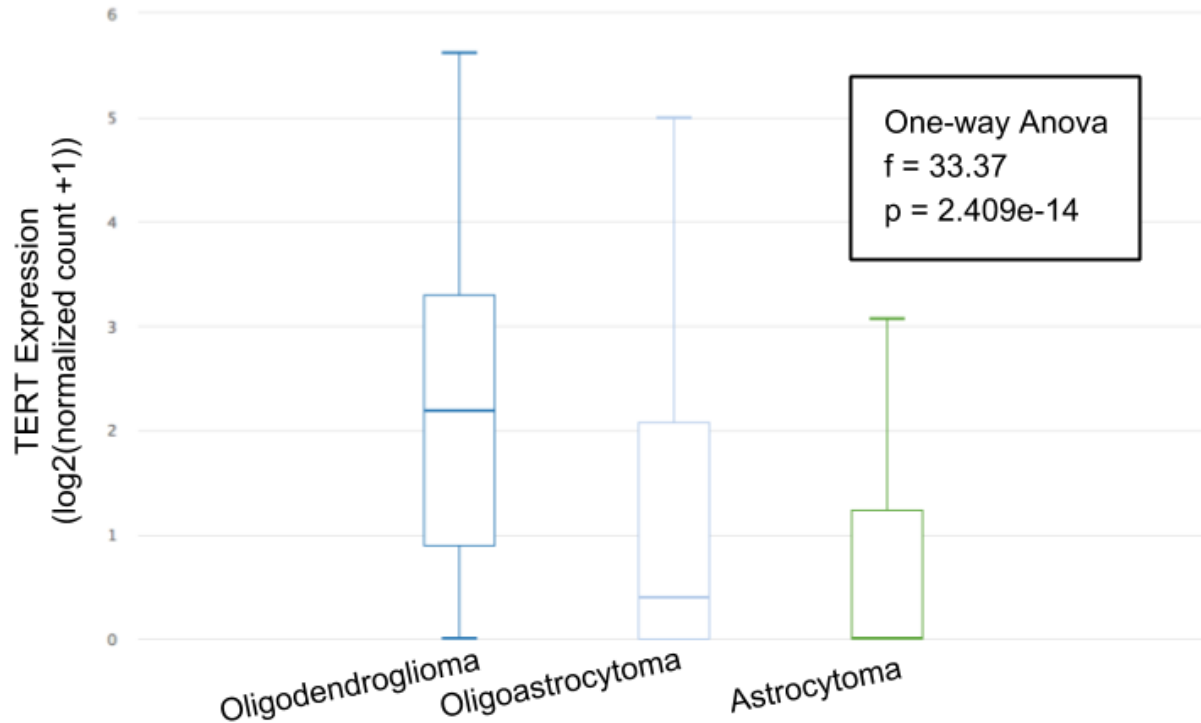
Supplemental Figure 2



Supplemental Figure 2. Visualization of both coding and non-coding mutations from a gene-centric perspective in ICGC lymphoma. The columns left to right are cancer type, *BCL2*, *BCL7A*, *BIRC3* and *ST6GAL1* mutation status, respectively. Gene diagrams are shown at the top of each column with exons in light and dark grey boxes with coding regions being taller and untranslated regions being shorter. The position of each mutation is marked in relation to the gene diagram and colored by its functional impact, with deleterious mutations in red, missense mutations and in-frame indels in blue, synonymous mutations in green, splice site mutations in orange, and mutations with an unknown functional impact in grey. This figure shows the frequent intronic mutations in these genes, which are visible via our dynamic toggle to show or hide introns. These mutation 'pile-ups' would not be visible if viewing exomes only. While the majority of the intronic mutations in this view have an unknown impact (shown in grey), they do overlap with known enhancer regions (Mathelier 2015).

<https://xenabrowser.net/heatmap/?bookmark=d2a79e46e22456036a732c49c2e4c5b3>

Supplemental Figure 3



Supplemental Figure 3. Xena Chart View showing a box plot of TERT expression for each of the TCGA lower grade glioma histological subtypes. Columns created in the Visual Spreadsheet (Figure 2) are used to construct the chart. Statistical analyses are automatically computed. This view shows a significant expression difference for TERT between oligodendroglioma, oligoastrocytoma and astrocytoma histologies (one-way ANOVA, $p < 0.05$).

<https://xenabrowser.net/heatmap/?bookmark=ae1a7f260e8d95bd3c1742503de32192>